Journal of Membrane Science 463 (2014) 134–144

Contents lists available at ScienceDirect

Journal of Membrane Science

journal homepage: www.elsevier.com/locate/memsci

Preparation and performance of different amino acids functionalized titania-embedded sulfonated poly (ether ether ketone) hybrid membranes for direct methanol fuel cells

Hong Wu [a,b,c], Ying Cao [a,b], Xiaohui Shen [a,b], Zhen Li [a,b], Tao Xu [a,b], Zhongyi Jiang [a,b,*]

[a] Collaborative Innovation Center of Chemical Science and Engineering (Tianjin), Tianjin 300072, China
[b] Key Laboratory for Green Chemical Technology, School of Chemical Engineering and Technology, Tianjin University, Tianjin 300072, China
[c] Tianjin Key Laboratory of Membrane Science and Desalination Technology, Tianjin University, Tianjin 300072, China

ARTICLE INFO

Article history:
Received 12 January 2014
Received in revised form
19 March 2014
Accepted 21 March 2014
Available online 1 April 2014

Keywords:
Amino acids
Titania submicrospheres
Sulfonated poly (ether ether ketone)
Hybrid membranes
Proton conductivity

ABSTRACT

A series of amino acid functionalized titania submicrospheres were synthesized and incorporated into sulfonated poly (ether ether ketone) (SPEEK) to fabricate organic–inorganic hybrid proton exchange membranes. Pristine TiO_2 with a uniform particle size of ~200 nm were synthesized and functionalized with four kinds of amino acids including oxidized L-cysteine, O-phospho-L-serine, aspartic acid and histidine, designated as TiO_2–Scys, TiO_2–Pser, TiO_2–Asp and TiO_2–His, respectively. The effects of amino acid attribute on the membrane properties were investigated. At the filler content of 15 wt%, the TiO_2–Scys embedded membrane exhibited the highest proton conductivity of about 5.98×10^{-3} S cm^{-1} (20 °C, 100% RH), while the TiO_2–His embedded membrane exhibited the lowest conductivity due to the strong acid-base interaction between the basic imidazole groups of histidine and the sulfuric acid groups of SPEEK. The TiO_2–Pser embedded membrane exhibited the highest selectivity of 17.10×10^3 S s cm^{-1}. In addition, the methanol crossover of the hybrid membranes was reduced by two folds, and the anti-swelling property and thermal stability of the hybrid membranes were also enhanced.

1. Introduction

Direct methanol fuel cells (DMFCs) as promising portable and transport power sources have drawn wide attention due to their high power density, low pollution, long life time and compact cell design [1,2]. Proton exchange membrane (PEM) is one of the key components of DMFCs. The current state-of-art PEMs represented by Nafion (Dupont) suffer from high cost, serious methanol crossover and proton conductivity loss at high temperature, thus hindering their practical application in DMFCs [2,3]. Membranes with enhanced proton conductivity, reduced methanol permeability and acceptable cost are required for DMFCs [4–6]. To meet these requirements, various approaches have been explored in recent years [7]. Among them, the employment of organic–inorganic hybrid PEMs seems attractive because of their ability to rationally combine the characters of organic moiety and inorganic moiety [8,9]. Incorporation of inorganic additives into polymers could endow the hybrid membranes with enhanced mechanical stability and better water-retaining property [6,10,11]. However, proton conductivity usually decreases with increasing filler content due to the rather low proton conductivity of inorganic additives and their considerable dilution effect on the proton conductive groups [12]. Anchoring extra proton-conducting groups, such as sulfonic acid group [13–15] and phosphonic acid group [16–19] *etc.*, onto the surface of inorganic particles could provide more facile hopping sites for protons, which in turn would help to increase the proton mobility, thus resulting in the enhancement of proton conductivity [10].

In living organisms, proton transfer plays a key role in the cellular energy interconversion which occurs along proton channels such as the M2 proton channel of influenza A virus [20], cytochrome–oxidase complex in mitochondria [21] and bacteriorhodopsin in Halobacterium [22]. Proton transfer operates very efficiently through these amino acid-lined channels, for example, 10^5 protons are conducted per second through one channel at a 100 mV potential drop in adenosine triphosphate (ATP) synthase systems [23]. Inspired by the proton conducting mechanism in organisms where each amino acid acts as acceptor and donor simultaneously in proton transfer, amino acids were introduced

Abbreviations: oxidized l-cysteine, Scys; O-phospho-l-serine, Pser; aspartic acid, Asp; histidine, His; sulfonation degree, DS; ion-exchange capacity, IEC; sulfonated poly(ether ether ketone), SPEEK

* Corresponding author at: Key Laboratory for Green Chemical Technology, School of Chemical Engineering and Technology, Tianjin University, Tianjin 300072, China. Tel./fax: +86 22 23500086.
E-mail address: zhyjiang@tju.edu.cn (Z. Jiang).

http://dx.doi.org/10.1016/j.memsci.2014.03.058
0376-7388/

into PEMs by many researchers. Hong Wu et al. [24] synthesized a series of titania submicrospheres grafted with various functional groups including amino acid group, amino group, carboxyl group and phenyl group, and incorporated them into sulfonated poly (ether ether ketone) (SPEEK) to fabricate hybrid membranes. Among all the membranes, the membranes embedded with amino acid functionalized TiO_2 displayed a superior proton-conducting ability. Leem et al. [23] attached different kinds of amino acids (L-lysine, aspartic acid, glutamic acid and methionin) to silica nanoparticles and incorporated them into porous membranes (polyethylene terephthalate, polycarbonate). No power output was observed in the absence of amino acids while a variable power output depending on the nature of the amino acids and the chemical addition was observed. These distinct differences were ascribed to the structure of the amino acids and the amino acid–water surface layer formed on nanoparticles.

Although it has been demonstrated that amino acids could mediate the transport of protons in PEMs, few efforts have been dedicated to investigate the influence of various kinds of amino acids on the membrane performance. In this study, four kinds of amino acids were selected for comparison, including oxidized L-cysteine, O-phospho-L-serine, aspartic acid and histidine. These four kinds of amino acids have similar structures with different end groups including sulfonic acid groups (strong acidic), phosphonic acid groups (mediate strong acidic), carboxyl groups (weak acidic) and imidazole groups (alkaline), exhibiting different capacity to donate or accept protons. A series of amino acid functionalized titania submicrospheres were synthesized and doped into SPEEK to fabricate hybrid proton conducting membranes for potential application in DMFCs. The as-prepared membranes were extensively evaluated in terms of swelling degree, water uptake, methanol permeability and proton conductivity.

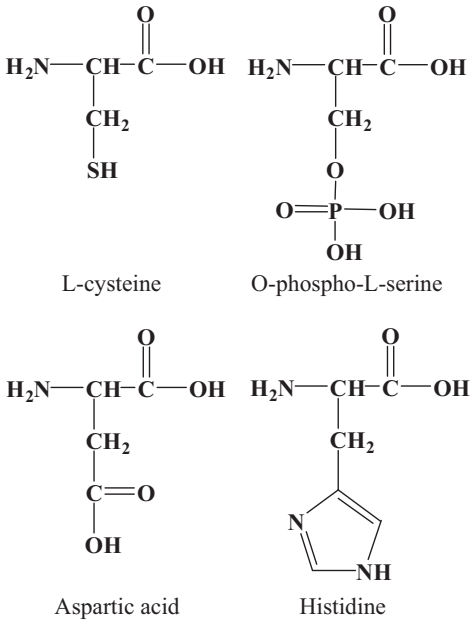

Scheme 1. Molecular structures of the modification reagents.

2. Experimental

2.1. Materials and chemicals

Poly (ether ether ketone) (PEEK) was purchased from Victrex High-performance Materials Co., Ltd. (Shanghai, China). 3-(3,4-dihydroxyphenyl) propionic acid was purchased from Alfa Aesar. Tetrabutyl titanate (TBT, > 98%), histidine, aspartic acid, L-cysteine, hydrochloric acid (HCl, 36%-38%) and N,N-Dimethylformamide (DMF, > 99.5%) from Tianjin Guangfu Fine Chemical Research Institute (Tianjin, China), and O-phospho-L-serine from Sigma-Aldrich were used as received without further purification.

2.2. Preparation of functionalized TiO_2 submicrospheres

Preparation of TiO_2 submicrospheres was carried out via a modified sol-gel method as described before [25]. For the carboxylation of TiO_2, a facile chelation procedure was conducted [26]. A certain amount of TiO_2 powders were suspended in hydrochloric acid aqueous solution (pH=2) under ultrasonic treatment for 2 h to break aggregates. The obtained solution was poured into a large excessive of 4 mg L^{-1} 3-(3,4-dihydroxyphenyl) propionic acid solution, followed by vigorous stirring for 0.5 h. The carboxyl functionalized TiO_2 submicrospheres were collected by centrifugation, washed with deionized water till neutral pH and dried overnight. The obtained TiO_2 submicrospheres were designated as TiO_2–Car. For modifying TiO_2 with amino acid, L-cysteine, O-phospho-L-serine, aspartic acid and histidine (molecular structures shown in Scheme 1) were used as modification reagents. 1.0 g of TiO_2–Car were added into 200 mL of 4-Morpholineethanesulfonic acid (MES, 50 mM, pH=6.5) under ultrasonic treatment for 15 min, and then 6 mmol of 1-(3-Dimethylaminopropyl)-3-ethylcarbodiimide hydrochloride (EDC) and 30 mmol of N-Hydroxysuccinimide (NHS) were added into the above solution under vigorous stirring at room temperature for 1 h to activate the carboxyl groups on TiO_2–Car [27]. After activation, the TiO_2–Car were washed with deionized water to remove the unreacted EDC and NHS, and collected by centrifugation. Then, the as-collected TiO_2–Car were suspended respectively in the MES solution of the four kinds of amino acid, and reacted under room temperature for 4 h, followed by centrifugal separation and washed to neutral pH. Herein, the obtained L-cysteine functionalized TiO_2 submicrospheres were treated with 1 wt% oxidize hydrogen for 24 h to get oxidized. The final obtained functionalized TiO_2 grafted respectively with oxidized L-cysteine, O-phospho-L-serine, aspartic acid, and histidine were designated as TiO_2–Scys, TiO_2–Pser, TiO_2–Asp, and TiO_2–His.

2.3. Sulfonation of PEEK

PEEK was firstly dried in oven at 80 °C for 24 h before sulfonation. Then, 28 g of dried PEEK was dissolved into 200 mL concentrated sulfuric acid (H_2SO_4, 95–98%) under vigorous stirring at room temperature for 4 h and then at 45 °C for 8 h. The obtained solution was added into a large excess of ice-cold water under continuous stirring. The white precipitate was removed and washed with deionized water until neutral pH to remove residual acid. The sulfonated polymer was dried at room temperature for 24 h followed by drying at 60 °C under vacuum [28]. The degree of sulfonation (DS) was determined to be 61% through titration method [29].

2.4. Preparation of hybrid membranes

1.2 g of SPEEK was dissolved in 8 g of DMF under stirring at room temperature. A specific amount of functionalized TiO_2 submicrospheres were dispersed into 4 g of DMF under ultrasonic treatment for 24 h. Then, the above two solutions were mixed and stirred for another 24 h. The resulting mixture was cast onto a clean glass plate, dried first at 60 °C for 12 h and then 80 °C for

another 12 h. Afterwards, the resultant membranes were peeled off and converted to the required acid form by immerging in 1 mol L^{-1} hydrochloric acid solution for 24 h and washed with deionized water several times until neutral pH. Finally, the membranes were dried under vacuum at 25 °C for 24 h. The as-prepared membranes were designated as SPEEK/TiO_2–*X*–*Y*, where *X* refers to different functional groups grafted on TiO_2, and *Y* refers to weight percentage of inorganic fillers relative to SPEEK.

2.5. Characterization

The morphology of the TiO_2 submicrospheres was characterized by transmission electron microscopy (TEM, JEOL), and the cross-sectional morphology of membranes was observed by scanning electron microscopy (SEM, PHILIPS-XL30) operated at 20 kV. The SEM samples were prepared by freeze-fracturing in liquid nitrogen, and subsequently coated with a thin layer of sputtered gold.

The surface chemical composition of the TiO_2 submicrospheres was monitored by X-ray photoelectron spectroscopy (XPS) using a PHI-1600 spectrometer with AL Kα radiation for excitation. Fourier transform infrared spectra (FTIR, 4000–400 cm^{-1}) were recorded on a Nicolet-560 instrument.

Thermo gravimetric analysis (TGA) was carried out on Pyris instrument from PerkinElmer Company in the temperature range of 30–800 °C with a heating rate of 10 °C min^{-1} under N_2 atmosphere. Before testing, all the membranes were dried under vacuum for 24 h.

2.6. Water uptake and swelling degree

Water uptake and swelling degree were measured by setting the mass and area difference between the dry and wet membranes. A piece of dry, rectangular-shaped membrane with a weight of W_d (g) and an area of A_d (cm^2) was soaked in 25 °C water for 24 h. The membrane was then wiped with blotting paper and both the mass (W_w) and size (A_w) were remeasured. Each membrane was measured three times with an error range of ±5%. The water uptake and swelling degree of membranes were calculated as follows:

$$\text{water uptake}\ (\%) = \frac{W_w - W_d}{W_d} \times 100\% \quad (1)$$

$$\text{swelling degree}\ (\%) = \frac{A_w - A_d}{A_d} \times 100\% \quad (2)$$

2.7. Methanol permeability

Methanol permeability (*P*, $cm^2\ s^{-1}$) was measured using a glass diffusion cell composed of two compartments with an identical volume of 30 mL. The membrane under test was vertically placed between the two compartments that were filled with water (compartment A) and 2 mol L^{-1} methanol solution (compartment B), respectively. Before each test, the membrane was fully hydrated in water for 24 h. The concentration of methanol in compartment A was measured every three minutes using a gas chromatography (Agilent 7820) equipped with a thermal conductivity detector (TCD) and a DB-624 column until a straight line of methanol concentration in compartment A along time was obtained. Both compartments were stirred continuously with a magnetic stirrer during the permeability test. The methanol permeability was

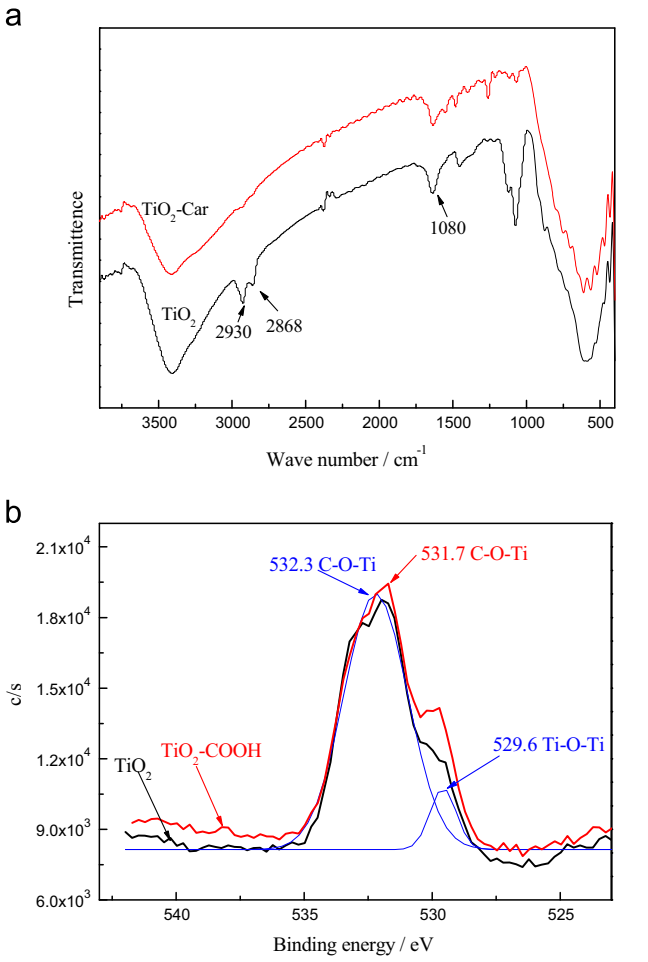

Fig. 2. FTIR spectra of TiO_2 and TiO_2–Car (a), XPS spectra of O (1s) of TiO_2 and TiO_2–Car (b).

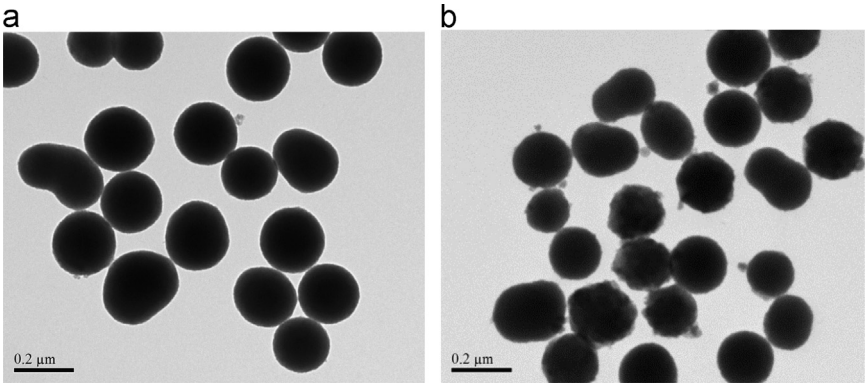

Fig. 1. TEM images of pristine TiO_2 (a), TiO_2–Car (b).

calculated by following equation,

$$P(\mathrm{cm^2\ s^{-1}}) = S\frac{V_A L}{AC_{B0}} \quad (3)$$

where S was the slope of the straight line of methanol concentration versus time in compartment A, and V_A (mL) was the volume of the receipt compartment. L (cm) and A (cm^2) were the membrane thickness and diffusion area, respectively. And C_{B0} (mol mL^{-1}) was the initial concentration of methanol in compartment B.

2.8. Ion exchange capacity (IEC)

The IEC value of the as-prepared membranes was measured with the back-titration method. Membranes in acid form were immersed in 20 mL of sodium chloride (NaCl) solution (2 mol L^{-1}) for about 24 h to replace H^+ with Na^+. Then the released H^+ was titrated with 0.01 mol L^{-1} sodium hydroxide (NaOH) using phenolphthalein as the indicator. The IEC value was calculated by following equation:

$$\mathrm{IEC\ (mmol\ g^{-1})} = \frac{0.01 \times 1000 \times V_{NaOH}}{W_d} \quad (4)$$

where V_{NaOH} (L) was the volume of NaOH consumed for titration and W_d (g) was the weight of dried membrane. Every sample was measured for three times.

2.9. Proton conductivity and selectivity

Proton conductivity measurement of membranes in the transverse direction was carried out on a two-point-probe conductivity cell, which was connected to a frequency response analyzer (Autolab PGSTAT20, Netherlands) at a frequency range of 1–1M Hz with an oscillating voltage of 20 mV. All of the membranes were soaked in deionized water for 24 h before test to get

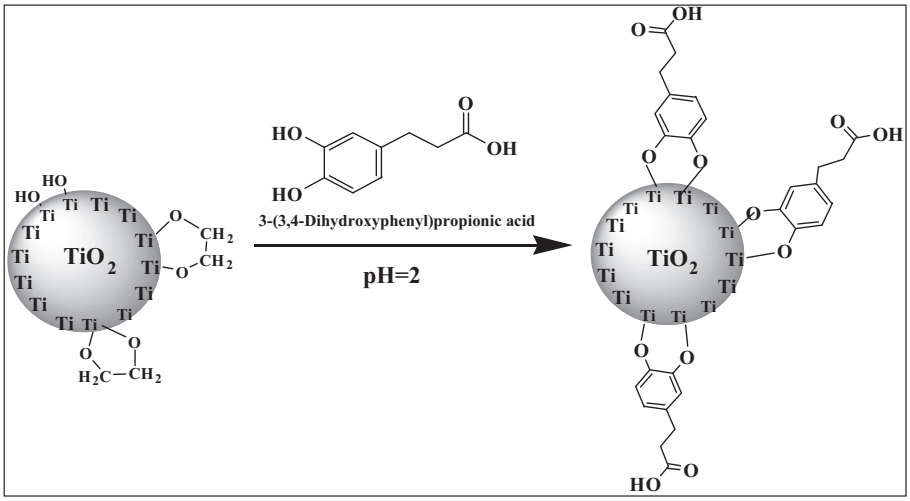

Scheme 2. Fabrication process of carboxyl acid functionalized TiO_2.

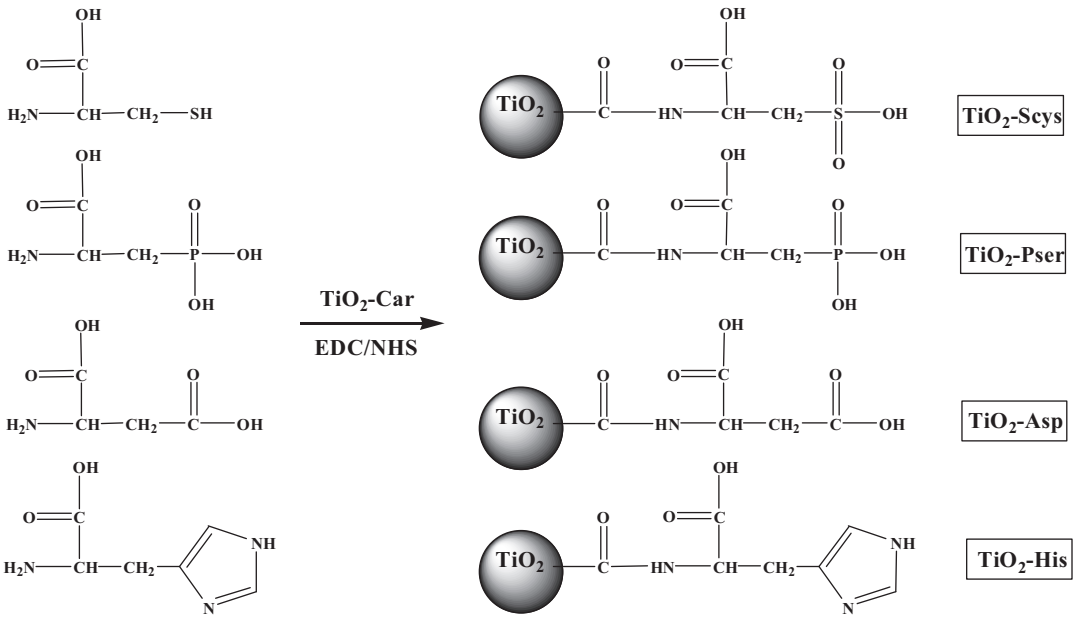

Scheme 3. Fabrication process of amino acid functionalized TiO_2.

fully hydrated. The proton conductivity was calculated as follow,

$$\sigma\ (S\ cm^{-1}) = \frac{l}{AR} \quad (5)$$

where l (cm) was the membrane thickness and A (cm^2) was the face area of membrane, while R (Ω) was the resistance derived from the low intersection of the high frequency semicircle on a complex impedance plane with Re(z) axis. Each membrane was measured for three times and took the average as final result.

The selectivity factor (β), defined as the ratio of proton conductivity to methanol permeability, was used as an indicator to evaluate the overall membrane property.

3. Results and discussion

3.1. Characterization of the TiO_2 submicrospheres

Fig. 1 showed the TEM images of pristine TiO_2 (Fig. 1(a)) and functionalized TiO_2–Car (Fig. 1(b)) submicrospheres. The unmodified TiO_2 particles were morphologically identical with an average particle size of ~200 nm. Compared with the unfunctionalized TiO_2 particles, the surface of the TiO_2–Car particles became rougher due to the aggregation of 3-(3,4-dihydroxyphenyl) propionic acid on the particle surface.

The surface composition and chemical structure of TiO_2–Car were confirmed using FTIR and XPS as shown in Fig. 2. Compared with the FTIR spectrum of pristine TiO_2, the characteristic peaks of ethylene glycol at 1080, 2868 and 2930 cm^{-1} disappeared after carboxylation, and the characteristic peaks of the functional groups appeared in the region of 1000–1500 cm^{-1} as shown in Fig. 2(a), confirming the successful modification of 3-(3,4-Dihydroxyphenyl) propionic acid on the surface of TiO_2. The high-resolution O (1s) XPS spectra of TiO_2 and TiO_2–Car were shown in Fig. 2(b). For pristine TiO_2, two peaks were detected: the strong one at 532.3 eV was attributed to the oxygen atom in C–O–Ti bond and the weak one at 529.6 eV was attributed to the oxygen atom in C–O–C bond. As for TiO_2–Car, the strong peak at 532.3 eV shifted to a lower binding energy (531.7 eV) by 0.6 eV, indicating that the original chelate positions of glycol were replaced by 3-(3,4-Dihydroxyphenyl) propionic acid through covalent bonds. Accordingly, the carboxylation process of TiO_2 was shown in Scheme 2.

TiO_2–Car were first activated by EDC/NHS chemistry, and then grafted with different kinds of amino acids (Scheme 3). In the FTIR spectra of amino acid functionalized TiO_2 (TiO_2–His, TiO_2–Scys, TiO_2–Asp and TiO_2–Pser), characteristic peaks of the amino acids appeared at 1000–1600 cm^{-1} (Fig. 3(a)). Moreover, the characteristic peaks of N (1s) and P (2p) appeared in the XPS spectra of TiO_2–His and TiO_2–Pser, respectively, which further confirmed the successful modification by amino acids (Fig. 3(b)).

To estimate the amounts of organics introduced on the surface of TiO_2, thermogravimetric analysis (TGA) was performed and shown in Fig. 4. The four kinds of amino acids functionalized TiO_2 had a similar degradation process composed of two main stages: the weight loss in the temperature range of 30–130 °C was attributed to the release of free and bond water in particles, and the weight loss starting from 300 °C was attributed to the thermal decomposition of amino acid molecules. Based on these data, the weight fraction of organics on TiO_2 particles was calculated to be 15–20%.

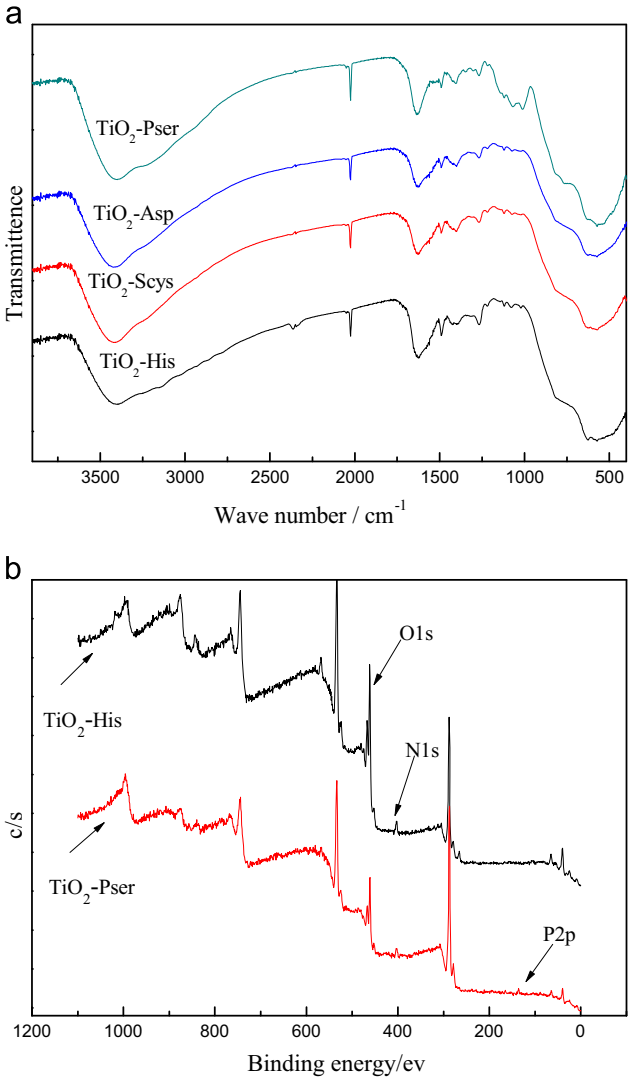

Fig. 3. FTIR spectra of amino acid functionalized TiO_2 (a), XPS spectra of N (1s) and P (2p) of amino acid functionalized TiO_2 (b).

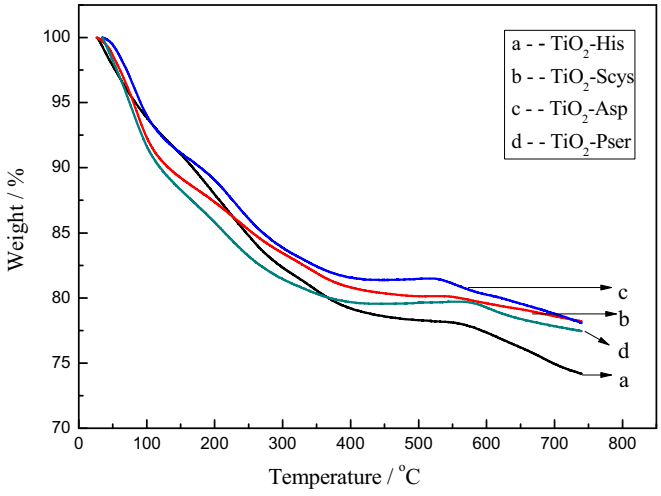

Fig. 4. TGA thermograms of amino acid functionalized TiO_2.

3.2. Characterization of hybrid membranes

The microstructure and dispersion status of functionalized TiO_2 in the membranes were confirmed by SEM. The cross-section images of the SPEEK/TiO_2–His hybrid membranes were shown in Fig. 5. The images demonstrated that the as-prepared TiO_2–His particles were dispersed homogeneously in SPEEK matrix without

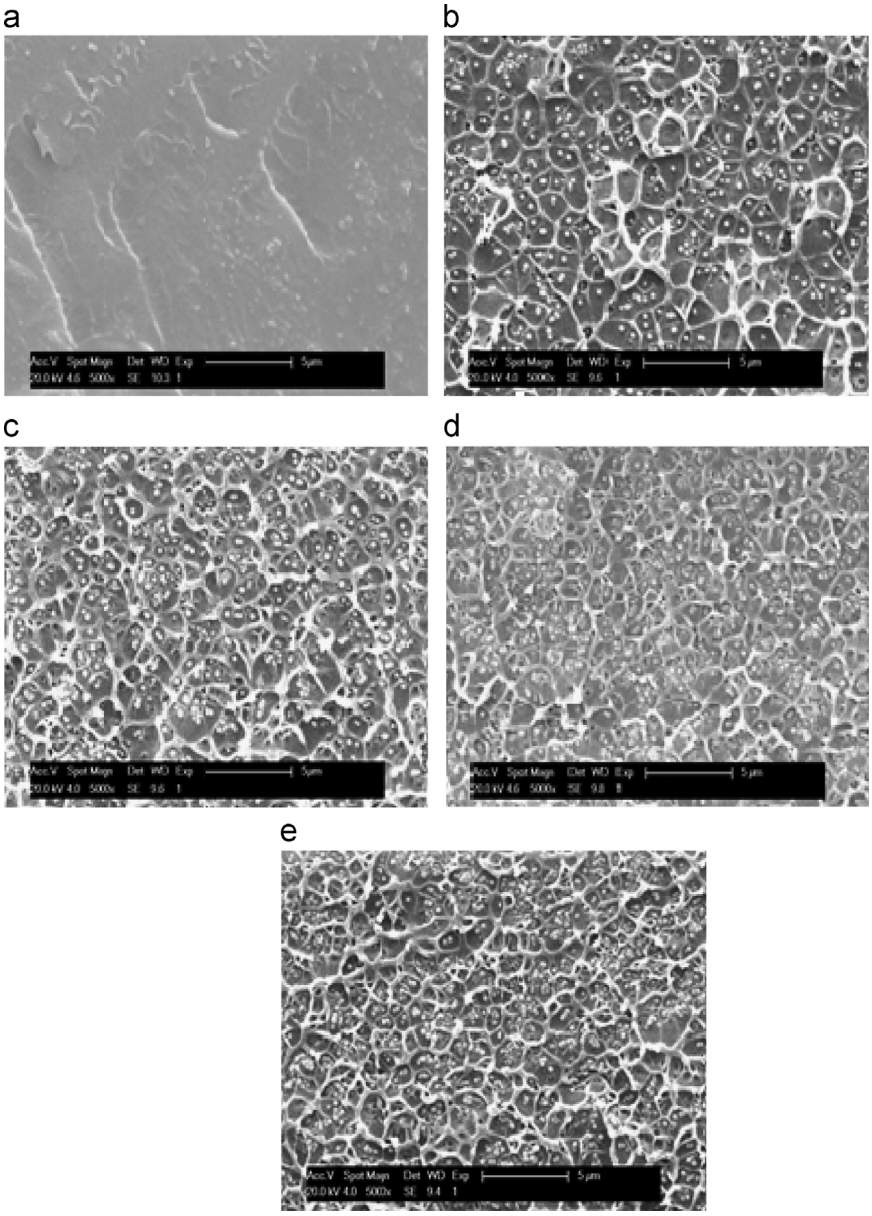

Fig. 5. SEM images of the cross-section of pristine SPEEK membrane and SPEEK/TiO_2–His.

any macroscopic structural defects when the filler content was less than 20 wt%. As for the SPEEK/TiO_2–His-20 membrane, slight agglomeration was observed. The morphologies of hybrid membranes containing TiO_2–Scys, TiO_2–Asp and TiO_2–Pser were similar with those shown in Fig. 5.

Since histine and O-phospho-L-serine both play important role in proton transfer process in biology, and their end groups (imidazole and phosphoric acid group) could donate and accept protons simultaneously, more detailed study was given on the membranes containing these amino acids. Fig. 6 showed the FTIR spectra of pristine SPEEK, SPEEK/TiO_2–His and SPEEK/TiO_2–Pser membranes. For pristine SPEEK membrane, the absorption bands at 1020, 1080 and 1253 cm^{-1} were assigned to asymmetric and symmetric stretching vibration of O═S═O and stretching vibration of S═O, respectively [14,19]. In the case of SPEEK/TiO_2–His and SPEEK/TiO_2–Pser membranes, the same bands were also presented while the intensity of the characteristic peaks of –SO_3H groups decreased due to the electrostatic force and hydrogen bonds between TiO_2–His/TiO_2–Pser and SPEEK [30].

3.3. Thermal stability of the hybrid membranes

The thermal stability of the as-prepared membranes was investigated through thermogravimetric analysis and the results were shown in Fig. 7. The TGA curves of all the membranes had a similar decomposition profile consisting of three major weight loss stages. The first weight loss at 30–50 °C was due to the evaporation of water and residual solvent within the membrane [31]. Herein, the SPEEK/TiO_2–Asp hybrid membranes exhibited a higher weight loss than other hybrid membranes in this stage, which might result from the larger hydration energy of carboxyl groups than that of other three functional groups. The second weight loss at 250–310 °C was attributed to the decomposition of functional groups on TiO_2 particles. The last mass loss at approximately

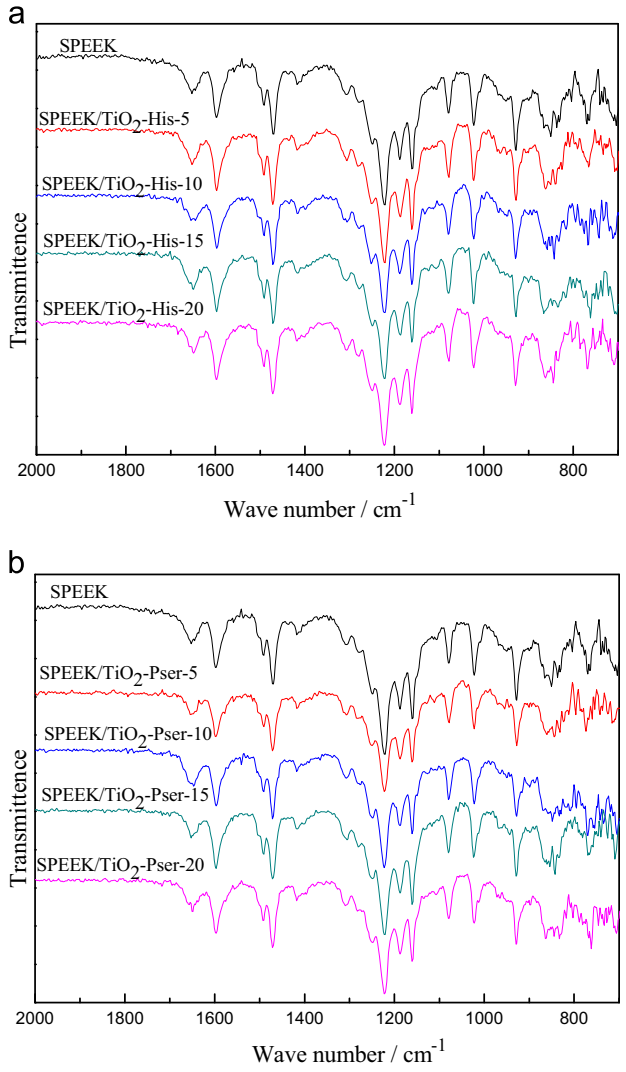

Fig. 6. FTIR spectra of pristine SPEEK membrane and SPEEK/TiO_2–His (a), SPEEK/TiO_2–Pser (b).

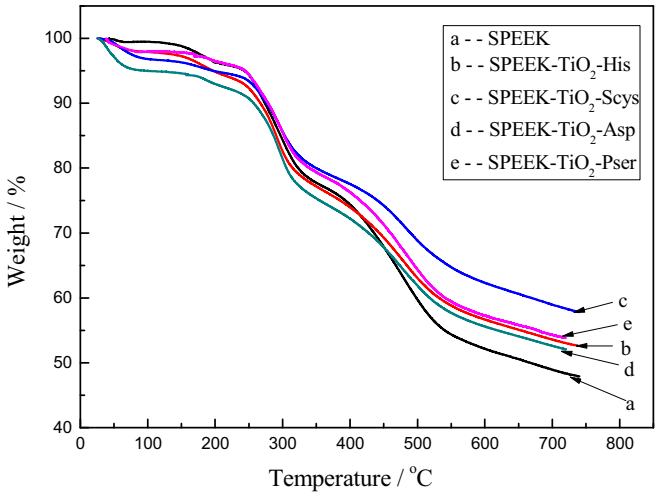

Fig. 7. TGA curves of pristine SPEEK membrane and hybrid membranes embedded with 15 wt% of amino acid functionalized TiO_2.

450 °C was ascribed to the decomposition of the polymer main chains [32,33]. Compared with the pristine SPEEK membrane, the hybrid membrane showed improved thermal stability. This indicated that the presence of inorganic fillers has restrained the mobility of polymer chains. It was notable that all the hybrid membranes were thermally stable below 250 °C, which could meet the thermal stability requirement for practical applications in DMFCs.

3.4. Swelling behavior of the hybrid membranes

The dimensional swelling behavior is one of the most important parameters of proton exchange membranes for DMFCs applications, especially for most sulfonic aromatic polymer membranes with high degree of sulfonation. High swelling degree might lead to obvious decrease of membrane performance, such as mechanical stability and methanol resistance [34,35]. The dimensional swelling degree of the as-prepared membranes were measured and presented in Fig. 8. As temperature increased, the swelling degree of all membranes increased. The incorporation of inorganic fillers has distinctly reduced the swelling degree of hybrid membranes. In addition, the swelling degree of hybrid membranes decreased with increasing filler content. As shown in Fig. 8(a), the swelling degree of the SPEEK/TiO_2–His membrane at 50 °C decreased from 68% to 39% as the filler content increased from 0 wt% to 20 wt%. This result can be rationalized by the reduced dimension of the ionic clusters and the strong interactions between TiO_2–His and SPEEK [36]. Fig. 8(c) showed the swelling degree of functionalized TiO_2 doped hybrid membranes at different temperatures with 15 wt% filler content. At the same temperature, the swelling degrees of the SPEEK/TiO_2–His, SPEEK/TiO_2–Scys and SPEEK/TiO_2–Pser membranes were lower than that of SPEEK/TiO_2 membrane. Among all the membranes, the SPEEK/TiO_2–His-15 membrane exhibited the lowest swelling degree, due to the electrostatic attraction between alkaline imidazole groups on TiO_2–His and sulfonic acid groups of SPEEK, which has further restrained the mobility of polymer chains [33]. Besides, due to the strong water affinity of carboxyl, the swelling degree of the SPEEK/TiO_2–Asp membrane was slightly higher than other hybrid membranes, but still much lower than that of SPEEK membrane.

3.5. Water uptake and methanol permeability

The water uptake and methanol permeability could greatly influence the performance of membranes in DMFCs [35]. Fig. 9 (a) showed the water uptake and methanol permeability of the pristine SPEEK and hybrid membranes (SPEEK/TiO_2–His and SPEEK/TiO_2–Pser). The water uptake of hybrid membranes was lower than that of pristine SPEEK membrane, as a result of the less hydrophilic character of TiO_2 compared with SPEEK (see Fig. 9(c)). With the filler content increased from 5 wt% to 20 wt%, the water uptake decreased slightly from 21 wt% to 17 wt% for SPEEK/TiO_2–His membrane, and from 18 wt% to 14 wt% for SPEEK/TiO_2–Pser membrane. The methanol permeability of pristine SPEEK membrane was 8.81×10^{-7} cm^2 s^{-1}, much higher than that of hybrid membranes. When the filler content was lower than 10 wt%, the methanol permeability of hybrid membranes incorporated with TiO_2–His or TiO_2–Pser decreased obviously with increasing filler content, while further increase of filler content caused a slighter decrease of methanol permeability (Fig. 9(a)). These results can be rationalized by the size reduction of the ionic channels, which was unfavorable for methanol crossover. In the case of SPEEK/TiO_2–His, the transport channels were further narrowed by the ionic bond between alkaline imidazole group on TiO_2–His and sulfonic group on SPEEK, thus both water uptake and methanol permeability of them were lower than other membranes. The methanol permeability of hybrid membranes incorporated with 15 wt% of amino acid functionalized TiO_2 was measured and presented in Fig. 9(b). Both water uptake and methanol permeability of SPEEK/TiO_2–Asp-15 were found

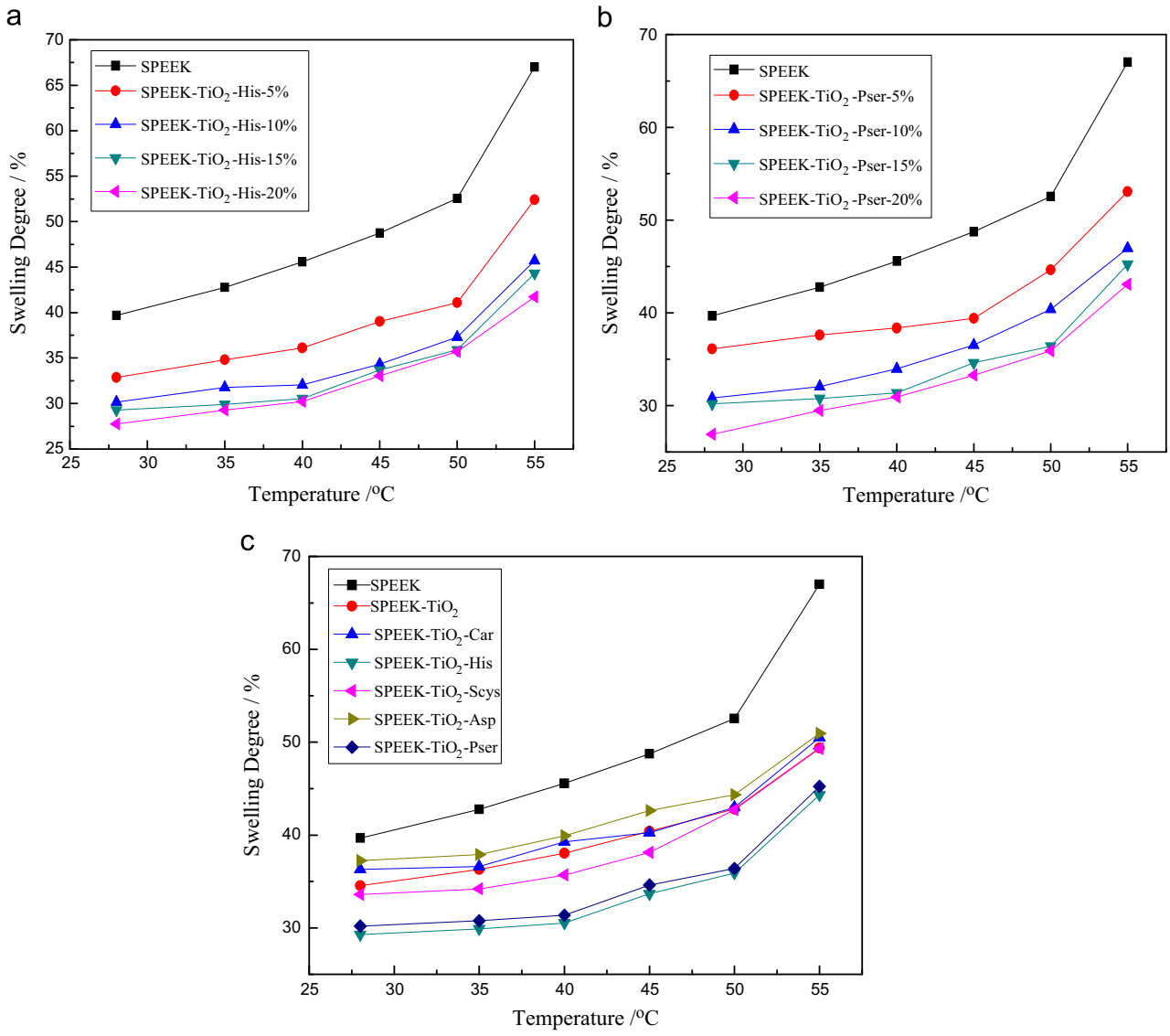

Fig. 8. Swelling degree of pristine SPEEK membrane and SPEEK/TiO_2–His (a), SPEEK/TiO_2–Pser (b), hybrid membranes embedded with 15 wt% of functionalized TiO_2 (c), at different temperatures.

to be higher than other hybrid membranes due to the more hydrophilic character of hydroxyl groups. All the as-prepared hybrid membranes exhibited improved methanol resistance compared with pristine SPEEK membrane.

3.6. IEC and proton conductivity

IEC is an indicator of the density of ionizable hydrophilic functional groups in the membrane and proton conductivity is a major parameter to evaluate the membrane performance. It was reported that there were two main mechanisms describing how proton diffused through the membranes. One was the "Grotthus mechanism" wherein the protons were transferred from one proton-conducting site to another by hydrogen bonds [37]. The other was the vehicle mechanism whereby protons combined with vehicles such as H_3O^+ or $H_5O_2^+$ [38]. The IEC values and proton conductivity of the as-prepared membranes measured at room temperature and 100% RH were shown in Table 1. The IEC and proton conductivity of pristine SPEEK membrane were respectively 1.81 mmol g^{-1} and 5.06×10^{-3} S cm^{-1}. After the incorporation of 15 wt% of pristine TiO_2, the IEC values and proton conductivity of the hybrid membranes both decreased. This finding could be ascribed to that the presence of pristine TiO_2 with poor proton-conducting ability has diluted the concentration of dissociable H^+ ions and increased the resistance of proton conduction.

In the case of SPEEK/TiO_2–Pser and SPEEK/TiO_2–His hybrid membranes, although their IEC values were lower than the pristine SPEEK membrane, their proton conductivity was increased. The incorporation of amino acid functionalized TiO_2 could introduce acid-base pairs as proton donors and acceptors into polymer, which help to form continuous pathways for proton hopping, thus leading to increased proton conductivity. Besides, the incorporation of proton donors and acceptors into membranes simultaneously could improve proton conductive property more efficiently than merely increase of IEC. As for the hybrid membranes incorporated with 15 wt% of amino acid functionalized TiO_2, the SPEEK/TiO_2–Scys-15 membrane with SO_3H-terminated amino acid showed the highest proton conductivity of 5.98×10^{-3} S cm^{-1}, followed by the SPEEK/TiO_2–Pser-15 membrane with phosphoric acid-terminated amino acid, about 5.90×10^{-3} S cm^{-1}, and the SPEEK/TiO_2–His-15 membrane embedded with the basic imidazole group-terminated amino acid exhibited the lowest proton conductivity of 5.09×10^{-3} S cm^{-1}. The order was in excellent

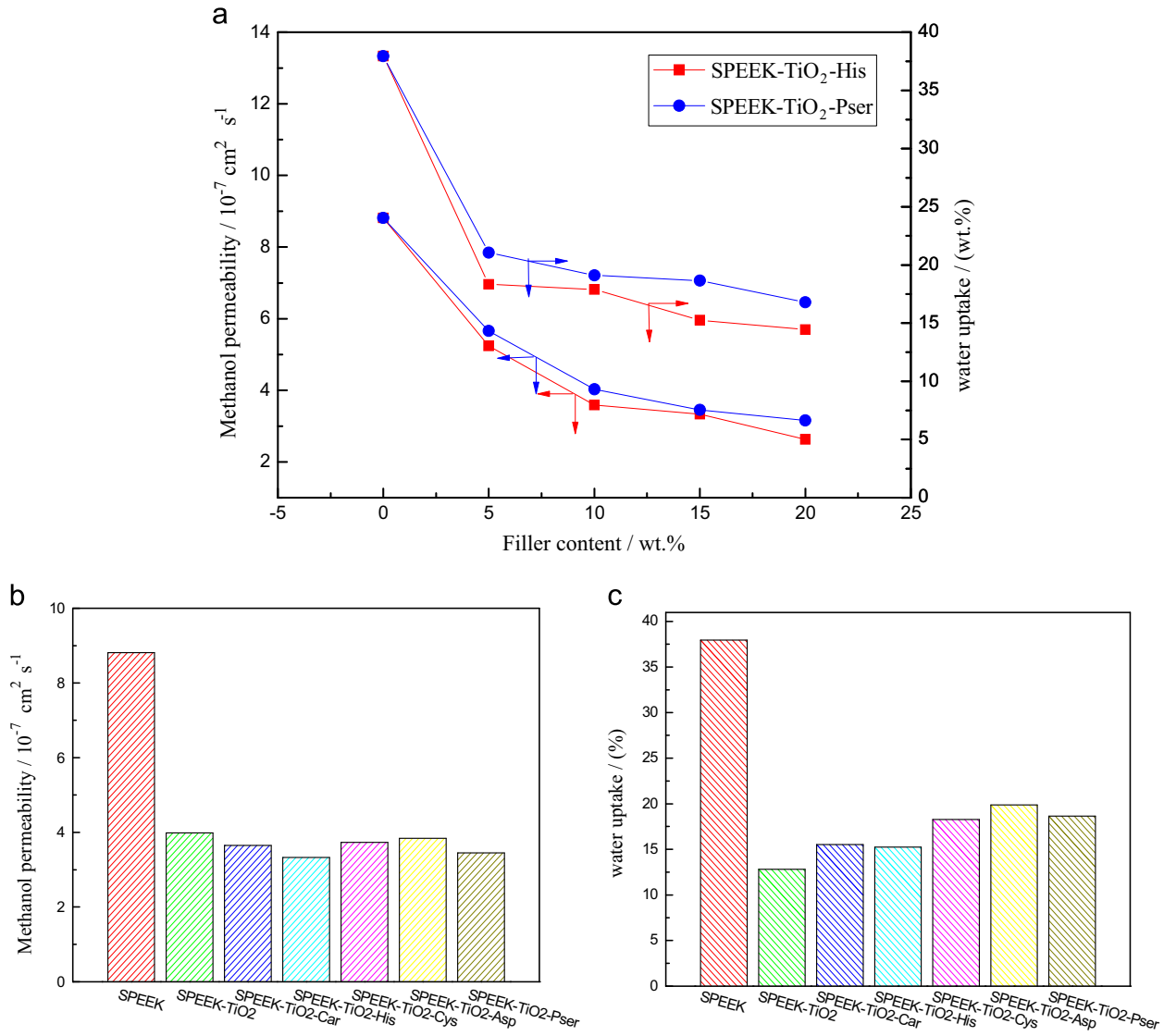

Fig. 9. Methanol permeability and water uptake of pristine SPEEK membrane and SPEEK/TiO_2–His and SPEEK/TiO_2–Pser(a), methanol permeability of pristine SPEEK membrane and hybrid membranes embedded with 15 wt% of functionalized TiO_2 (b), water uptake of SPEEK and hybrid membranes embedded with 15 wt% of functionalized TiO_2 (c).

agreement with the change tendency of IEC values of these membranes and revealed that the proton conductivity was negatively correlated with the acid dissociation constant (pKa) of amino acid end groups.

Fig. 10 showed the IEC values and proton conductivity of the SPEEK/TiO_2–His membrane and the SPEEK/TiO_2–Pser membrane with different filler contents. The IEC values of these membranes were decreased with increasing filler content. Meanwhile, their proton conductivity increased as the filler content increasing from 0 wt% to 10 wt%, and a decrease was observed when the filler content was more than 10 wt%. The proton conductivity decline might result from the agglomeration of functionalized TiO_2 particles. It was obviously that the proton conduction property of hybrid membranes could be influenced by the concentration of amino acids. Additionally, both the IEC values and proton conductivity of the SPEEK/TiO_2–His membrane were lower than those of the SPEEK/TiO_2–Pser membrane. Herein, the SPEEK/TiO_2–Pser-10 membrane showed the highest proton conductivity and selectivity among all the as-prepared membranes of 7.37×10^{-3} S cm^{-1} and 18.29×10^3 S s cm^{-1}.

4. Conclusions

In this study, TiO_2 submicrospheres were synthesized *via* a modified sol-gel method and functionalized with four kinds of amino acids including oxidized L-cysteine, O-phospho-L-serine, aspartic acid and histidine. These submicrospheres were incorporated into SPEEK matrix to fabricate hybrid membranes. The presence of pristine TiO_2 submicrospheres has reduced the size of the transport channels, leading to decreased proton conductivity and methanol permeability. After the incorporation of amino acid functionalized TiO_2, continuous pathways for proton conduction were formed inside the membranes, thus enhancing the proton conductivity. At the filler content of 15 wt%, the proton conductivity of hybrid membranes was increased in the following order: SPEEK/TiO_2–Scys > SPEEK/TiO_2–Pser > SPEEK/TiO_2–Asp > SPEEK/TiO_2–His, while the SPEEK/TiO_2–Pser membrane displayed the highest selectivity of 17.10×10^3 S s cm^{-1}. The reason for these differences was related to the different proton acceptor-donor capability of amino acids, and the proton conductivity of hybrid membranes was negatively correlated with the pKa of amino acid end groups. It was reasonable to conclude that high performance of

Table 1
IEC values, proton conductivity, methanol permeability and selectivity of SPEEK and hybrid membranes.

Membrane	IEC (mmol g^{-1})	σ (10^{-3} S cm^{-1})	P (10^{-7} cm^2 s^{-1})	β (10^3 S s cm^{-3})
SPEEK	1.81	5.06	8.81	5.74
SPEEK–TiO_2–15	1.57	3.96	3.99	9.92
SPEEK–TiO_2–Pser-5	1.76	5.92	5.66	10.46
SPEEK–TiO_2–Pser-10	1.73	7.37	4.03	18.29
SPEEK–TiO_2–Pser-15	1.69	5.90	3.45	17.10
SPEEK–TiO_2–Pser-20	1.54	4.18	3.16	13.23
SPEEK/TiO_2–His-5	1.73	5.30	5.24	10.11
SPEEK/TiO_2–His-10	1.67	6.16	3.59	17.16
SPEEK/TiO_2–His-15	1.60	5.09	3.33	15.29
SPEEK/TiO_2–His-20	1.50	3.95	2.63	15.02
SPEEK/TiO_2–Car-15	1.61	5.61	3.65	15.37
SPEEK/TiO_2–Scys-15	1.76	5.98	3.73	16.03
SPEEK/TiO_2–Asp-15	1.67	5.19	3.84	13.52

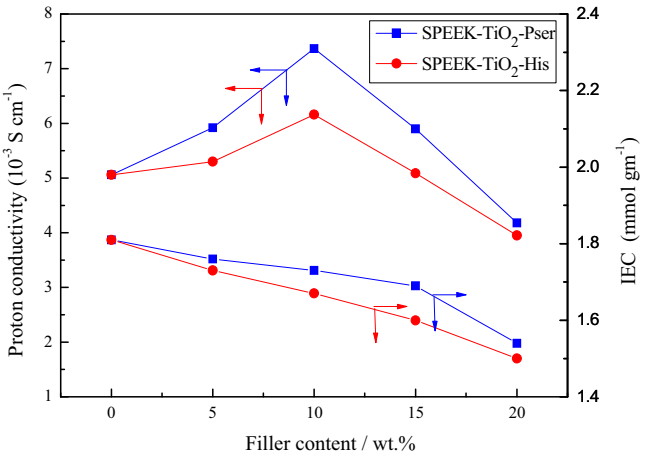

Fig. 10. The IEC values and proton conductivity of pristine SPEEK membrane, SPEEK/TiO_2–His and SPEEK/TiO_2–Pser.

hybrid PEMs could be acquired by embedding different amino acids functionalized inorganic fillers to tune the characters of channels/pathways for proton conduction and methanol diffusion.

Acknowledgment

The authors gratefully acknowledge financial support from Program for New Century Excellent Talents in University (NCET-10-0623), the National Science Fund for Distinguished Young Scholars (21125627) and the Programme of Introducing Talents of Discipline to Universities (No. B06006).

Nomenclature

Symbols

Y	mass ratio of inorganic fillers to SPEEK (wt%)
W	mass of membrane (g)
A	effective membrane area (cm^2)
P	methanol permeability (cm^2 s^{-1})
S	slope of straight-line of methanol concentration in receipt compartment versus permeation time
V_A	volume of receipt compartment (cm^3)
L	membrane thickness (cm)
C_{B0}	feed concentration (mol mL^{-1})
V_{NaOH}	volume of consumed NaOH solution (mL)
σ	proton conductivity (S cm^{-1})
l	distance between two probes (cm)
R	membrane resistance (S^{-1})
β	selectivity factor, the ratio of proton conductivity to methanol permeability (S s cm^{-1})

Subscripts

d	dry membrane
w	wet membrane

References

[1] J. Jagur-Grodzinski, Polymeric materials for fuel cells: concise review of recent studies, Polym. Adv. Technol. 18 (2007) 785–799.
[2] H. Zhang, P.K. Shen, Recent development of polymer electrolyte membranes for fuel cells, Chem. Rev. 112 (2012) 2780–2832.
[3] G.L. Athens, Y. Ein-Eli, B.F. Chmelka, Acid-functionalized mesostructured aluminosilica for hydrophilic proton conduction membranes, Adv. Mater. 19 (2007) 2580–2587.
[4] H. Ahmad, S.K. Kamarudin, U.A. Hasran, W.R.W. Daud, Overview of hybrid membranes for direct-methanol fuel-cell applications, Int. J. Hydrogen Energy 35 (2010) 2160–2175.
[5] S.J. Peighambardoust, S. Rowshanzamir, M. Amjadi, Review of the proton exchange membranes for fuel cell applications, Int. J. Hydrogen Energy 35 (2010) 9349–9384.
[6] B.C.H. Steele, A. Heinzel, Materials for fuel-cell technologies, Nature 414 (2001) 345–352.
[7] F. Lufrano, V. Baglio, P. Staiti, V. Antonucci, A.S. Arico, Performance analysis of polymer electrolyte membranes for direct methanol fuel cells, J. Power Sources 243 (2013) 519–534.
[8] B.P. Tripathi, V.K. Shahi, Organic–inorganic nanocomposite polymer electrolyte membranes for fuel cell applications, Prog. Polym. Sci. 36 (2011) 945–979.
[9] C. Sanchez, F. Ribot, Design of hybrid organic–inorganic materials synthesized via sol–gel chemistry, New J. Chem. 18 (1994) (1987) 1007–1047.
[10] R. Kannan, B.A. Kakade, V.K. Pillai, Polymer electrolyte fuel cells using nafion-based composite membranes with functionalized carbon nanotubes, Angew. Chem. Int. Ed. 47 (2008) 2653–2656.
[11] C. Yang, S. Srinivasan, A.B. Bocarsly, S. Tulyani, J.B. Benziger, A comparison of physical properties and fuel cell performance of Nafion and zirconium phosphate/Nafion composite membranes, J. Membr. Sci. 237 (2004) 145–161.
[12] D. Marani, A. D'Epifanio, E. Traversa, M. Miyayama, S. Licoccia, Titania Nanosheets (TNS)/Sulfonated Poly Ether Ether Ketone (SPEEK) nanocomposite proton exchange membranes for fuel cells, Chem. Mater. 22 (2009) 1126–1133.
[13] B.A. Holmberg, X. Wang, Y.S. Yan, Nanocomposite fuel cell membranes based on Nafion and acid functionalized zeolite beta nanocrystals, J. Membr. Sci 320 (2008) 86–92.
[14] T. Xu, W. Hou, X. Shen, H. Wu, X. Li, J. Wang, Z. Jiang, Sulfonated titania submicrospheres-doped sulfonated poly(ether ether ketone) hybrid membranes with enhanced proton conductivity and reduced methanol permeability, J. Power Sources 196 (2011) 4934–4942.
[15] Z. Jiang, X. Zhao, Y. Fu, A. Manthiram, Composite membranes based on sulfonated poly (ether ether ketone) and SDBS-adsorbed graphene oxide for direct methanol fuel cells, J. Mater. Chem. 22 (2012) 24862–24869.

[16] Y. Jin, S.Z. Qiao, J.C.D. da Costa, B.J. Wood, B.P. Ladewig, G.Q. Lu, Hydrolytically stable phosphorylated hybrid silicas for proton conduction, Adv. Funct. Mater. 17 (2007) 3304–3311.
[17] S. Sugata, S. Suzuki, M. Miyayama, E. Traversa, S. Licoccia, Effects of tin phosphate nanosheet addition on proton-conducting properties of sulfonated poly(ether sulfone) membranes, Solid State Ion. 228 (2012) 8–13.
[18] W.H.J. Hogarth, J.C.D. da Costa, J. Drennan, G.Q. Lu, Proton conductivity of mesoporous sol-gel zirconium phosphates for fuel cell applications, J. Mater. Chem. 15 (2005) 754–758.
[19] H. Wu, W. Hou, J. Wang, L. Xiao, Z. Jiang, Preparation and properties of hybrid direct methanol fuel cell membranes by embedding organophosphorylated titania submicrospheres into a chitosan polymer matrix, J. Power Sources 195 (2010) 4104–4113.
[20] J.R. Schnell, J.J. Chou, Structure and mechanism of the M2 proton channel of influenza A virus, Nature 451 (2008) 591–595.
[21] K. Faxen, G. Gilderson, P. Adelroth, P. Brzezinski, A mechanistic principle for proton pumping by cytochrome c oxidase, Nature 437 (2005) 286–289.
[22] F. Garczarek, K. Gerwert, Functional waters in intraprotein proton transfer monitored by FTIR difference spectroscopy, Nature 439 (2006) 109–112.
[23] H.-J. Leem, I. Dorbandt, J. Rojas-Chapana, S. Fiechter, H. Tributsch, Bio-analogue amino acid-based proton-conduction wires for fuel cell membranes, J. Phys. Chem. C 112 (2008) 2756–2763.
[24] H. Wu, X. Shen, T. Xu, W. Hou, Z. Jiang, Sulfonated poly(ether ether ketone)/amino-acid functionalized titania hybrid proton conductive membranes, J. Power Sources 213 (2012) 83–92.
[25] X.C. Jiang, T. Herricks, Y.N. Xia, Monodispersed spherical colloids of titania: synthesis, characterization, and crystallization, Adv. Mater. 15 (2003) 1205–1209.
[26] R. Rodriguez, M.A. Blesa, A.E. Regazzoni, Surface complexation at the TiO_2(anatase)/aqueous solution interface: chemisorption of catechol, J. Colloid Interface Sci. 177 (1996) 122–131.
[27] S. Sam, L. Touahir, J. Salvador Andresa, P. Allongue, J.N. Chazalviel, A.C. Gouget-Laemmel, C. Henry de Villeneuve, A. Moraillon, F. Ozanam, N. Gabouze, S. Djebbar, Semiquantitative study of the EDC/NHS activation of acid terminal groups at modified porous silicon surfaces, Langmuir 26 (2009) 809–814.
[28] C.V. Mahajan, V. Ganesan, Atomistic simulations of structure of solvated sulfonated poly(ether ether ketone) membranes and their comparisons to nafion: I. Nanophase segregation and hydrophilic domains, J. Phys. Chem. B 114 (2010) 8357–8366.
[29] L. Li, J. Zhang, Y. Wang, Sulfonated poly(ether ether ketone) membranes for direct methanol fuel cell, J. Membr. Sci. 226 (2003) 159–167.
[30] Y. Zhao, Z. Jiang, D. Lin, A. Dong, Z. Li, H. Wu, Enhanced proton conductivity of the proton exchange membranes by the phosphorylated silica submicrospheres, J. Power Sources 224 (2013) 28–36.
[31] M.N.A.M. Norddin, A.F. Ismail, D. Rana, T. Matsuura, S. Tabe, The effect of blending sulfonated poly(ether ether ketone) with various charged surface modifying macromolecules on proton exchange membrane performance, J. Membr. Sci. 328 (2009) 148–155.
[32] S. Xue, G. Yin, Proton exchange membranes based on poly(vinylidene fluoride) and sulfonated poly(ether ether ketone), Polymer 47 (2006) 5044–5049.
[33] H. Wu, X. Shen, Y. Cao, Z. Li, Z. Jiang, Composite proton conductive membranes composed of sulfonated poly(ether ether ketone) and phosphotungstic acid-loaded imidazole microcapsules as acid reservoirs, J. Membr. Sci. 451 (2014) 74–84.
[34] T.J. Peckham, S. Holdcroft, Structure–morphology–property relationships of non-perfluorinated proton-conducting membranes, Adv. Mater. 22 (2010) 4667–4690.
[35] G. Gebel, Structure of membranes for fuel cells: SANS and SAXS analyses of sulfonated PEEK membranes and solutions, Macromolecules 46 (2013) 6057–6066.
[36] J. Wang, H. Zhang, Z. Jiang, X. Yang, L. Xiao, Tuning the performance of direct methanol fuel cell membranes by embedding multifunctional inorganic submicrospheres into polymer matrix, J. Power Sources 188 (2009) 64–74.
[37] N. Agmon, The Grotthuss mechanism, Chem. Phys. Lett. 244 (1995) 456–462.
[38] K.-D. Kreuer, A. Rabenau, W. Weppner, Vehicle mechanism, a new model for the interpretation of the conductivity of fast proton conductors, Angew. Chem. Int. Ed. 21 (1982) 208–209.